DOI: 10.1007/s10535-016-0599-1 BIOLOGIA PLANTARUM 60 (2): 343-354, 2016

The basis of pod dehiscence: anatomical traits of the dehiscence zone and expression of eight pod shatter-related genes in four species of *Brassicaceae*

Y. ZHANG[1], Y.Y. SHEN[1], X.M. WU[2], and J.B. WANG[1]*

College of Life Sciences, Wuhan University, Wuhan 430072, P.R. China[1]
Key Laboratory of Biology and Genetic Improvement of Oil Crops, Ministry of Agriculture, Wuhan 430062, P.R. China[2]

Abstract

Members of the *Brassicaceae* family disperse their seeds through a mechanism commonly referred to as fruit dehiscence or pod shatter. Pod shatter is influenced by variations in valve margin structure and by the molecular control pathways related to valve development. Anatomical patterns of the dehiscence zone from *Brassica napus* L., *Brassica rapa* L., *Brassica carinata* L., and *Sinapis alba* L., representing fruit types differing in pod shatter resistance, were compared using histological staining. The pod shatter-susceptible plant *B. napus* showed an increased lignin deposition at the vascular bundle of the replum as well as an increased separation of cell layers. In pod shatter-resistant plants *S. alba*, *B. rapa*, and *B. carinata*, we observed two layers of lignified valve margin cells. From these four species, we isolated and identified homologs of *SHATTERPROOF* (*SHP1*, *SHP2*), *INDEHISCENT* (*IND*), *ALCATRAZ* (*ALC*), *FRUITFULL* (*FUL*), *AGAMOUS* (*AG*), *NAC SECONDARY WALL THICKENING PROMOTING FACTOR1* (*NST1*), and *SEEDSTICK* (*STK*) genes involved in fruit development and pod shatter in *Arabidopsis*. Transcriptional analysis of these eight genes was performed by real-time polymerase chain reaction and the results demonstrate that differences in the expression patterns of the eight genes may be associated with dehiscence variation within these four species.

Additional key words: *Brassica carinata*, *B. napus*, *B. rapa*, fruit development, lignin, *Sinapis alba*.

Introduction

Fruit-bearing plants have evolved several mechanisms to effectively disperse their seeds and optimize survival of the following generation. These mechanisms often involve the formation of specific tissues that allow the fruit to efficiently release seeds at maturity (Dinneny and Yanofsky 2005). Many fruits of *Brassicaceae* species, including *Arabidopsis thaliana* and important *Brassica* crops, undergo a process commonly referred to as fruit dehiscence or pod shatter to achieve seed dispersal (Spence *et al.* 1996). In *Arabidopsis*, the fruit is a typical dehiscent silique and the region of the fruit that encloses the seeds is composed of three major distinct tissues: the valves or carpel walls, the central replum, and the valve margin at the valve-replum border where fruit opening takes place (Liljegren *et al*. 2000). In the mature and dry fruit, a lignified valve margin layer and a separation layer composed of a dehiscence zone in the valve margin and a single lignified cell layer in the valves called endocarp *b* produce spring-like tension, which allows the fruit to open after secreted cell wall-degrading hydrolytic enzymes initiate cell-cell separation events at the separation layer (Dinneny and Yanofsky 2005). However, pod shatter is an undesirable characteristic in domesticated crop plants, such as peas, beans, and *Brassica* oil crops, as it decreases yield due to seed loss during harvesting (Spence *et al*. 1996, Martinez-Andujar *et al*. 2012). For *B. napus*, the seed yield loss can be as high as 20 % of the harvest as result of unsynchronized maturation, and losses can reach 50 % when adverse conditions delay harvesting (Wang *et al*. 2007). Therefore, resistance to pod shatter is an important trait for agricultural crop improvement (Dinneny and Yanofsky 2005, Kadkol 2009).

Pod shatter is the result of an orchestrated series of events, including programmed cell fate differentiation and

Submitted 1 January 2015, *last revision* 15 September 2015, *accepted* 15 October 2015.
Abbreviations: *AG* - *AGAMOUS; ALC* - *ALCATRAZ*; DZ - dehiscence zone; *FUL* - *FRUITFULL*; *IND* - *INDEHISCENT*; NCBI - National Center for Biotechnology Information; *NST1* - *NAC SECONDARY WALL THICKENING PROMOTING FACTOR1*; RT-qPCR - real-time quantitative polymerase chain reaction; *SHP* - *SHATTERPROOF*; *STK* - *SEEDSTICK*.
Acknowledgments: This work was supported by the National Natural Science Foundation of China (31370258).
* Corresponding author; fax: (+86) 27 68752213, e-mail: jbwang@whu.edu.cn

mechanical processes at the valve margin (Ferrándiz 2002). Several genes encoding transcription factors required for development and dehiscence of fruits in *Arabidopsis* have been well characterized at the molecular level (Dinneny and Yanofsky 2005, Roeder and Yanofsky 2006). Several MADS-box genes, including *AGAMOUS* (*AG*), *SHATTERPROOF1* (*SHP1*), *SHATTERPROOF2* (*SHP2*), and *SEEDSTICK* (*STK*), have partially redundant roles in specifying carpel identity and may function together in a transcriptional complex (Pinyopich *et al*. 2003). The AG acts upstream of the transcriptional cascades, which regulates carpel identity and endocarp formation and positively regulates *SHP1* and *SHP2* (Favaro 2003). The *SHP1* and *SHP2* are known to promote carpel identity (Pinyopich *et al*. 2003), and also play a role in valve margin formation and dehiscence (Liljegren *et al*. 2000). Valve margin formation requires two other genes, *INDEHISCENT* (*IND*) and *ALCATRAZ* (*ALC*), which play roles downstream of the *SHP* genes. The *IND* encodes a basic helix-loop-helix (bHLH) protein (Liljegren *et al*. 2004) and *ALC* encodes a myc/bHLH protein (Rajani and Sundaresan 2001). The *IND* specifies valve margin cell fate and represses replum formation (Girin *et al*. 2010), and the combined actions of *IND* and *ALC* promote separation layer formation (Liljegren *et al*. 2004). Mutants defective in any of these genes fail to undergo valve margin formation and instead generate indehiscent fruits with the seeds trapped inside (Rajani and Sundaresan 2001, Liljegren *et al*. 2004). Together, *SHP1*, *SHP2*, *IND*, and *ALC* genes form a regulatory network that orchestrates differentiation of the valve margin; expression of valve margin identity genes is limited to the valve margin due to negative regulation by the MADS-box gene *FRUITFULL* (*FUL*) expressed in the valve (Liljegren *et al*. 2004). In *ful* mutants, the valves are composed with the valve margin cells (Ferrandiz *et al*. 2000). Mitsuda and Ohme-Takagi (2008) demonstrated that *NAC SECONDARY WALL THICKENING PROMOTING FACTOR1* (*NST1*) also plays a role in pod shatter by promoting secondary wall formation in valve margins and endocarp cells which are required for silique dehiscence in *Arabidopsis*. In *nst1* mutants, specific loss of secondary walls is evident at the valve margins resulting in indehiscent siliques. *SEEDSTICK* (*STK*, also known as *AGL11*) is required for normal seed shedding, and *stk* mutant siliques fail to detach seeds or retain them for an extended period as they do not produce a clear abscission zone (Pinyopich *et al*. 2003). Antagonistic activities of these genes determine fruit patterning in *Arabidopsis* (Gonzalez-Reig *et al*. 2012).

The molecular mechanism of pod shatter in *Arabidopsis* provides a valuable genetic basis for pod shatter resistance in other *Brassicaceae* species. It has previously been shown that ectopic expression of the *Arabidopsis FUL* gene by the 35S promoter in *B. juncea* can produce indehiscent siliques; nevertheless, pod shatter is difficult to control because of the strong nature of indehiscent phenotypes (Østergaard *et al*. 2006). Girin *et al*.（2010）demonstrated that fine-tuning the expression of the valve margin identity gene *IND* in *Brassica* can optimize dehiscence and yield a potentially useful partial dehiscence phenotype. *B. napus*, *B. rapa*, and *B. carinata* are important *Brassica* crop plants, and *Sinapis alba* is a closely related genus in the *Brassicaceae* family. It is known that *B. napus* is susceptible to pod shatter, whereas *B. carinata* and *B. rapa* are shatter-resistant, and *S. alba* is highly shatter-resistant with no yield loss caused by pod shatter (Spence *et al*. 1996, Wang *et al*. 2007). Previous studies have focused on the comparison of valve margin gene expression between dehiscent fruit containing a dehiscence zone and indehiscent fruit lacking a dehiscence zone (Liljegren *et al*. 2000, 2004, Avino *et al*. 2012, Lenser and Theißen 2013, Mühlhausen *et al*. 2013), and little is known regarding the valve margin identity genes from *B. napus*, *B. rapa*, *B. carinata*, and *S. alba*, representing fruit types differing in pod shatter resistance, which all form a dehiscence zone. Characterizing this diversity could increase our understanding of how the transcriptional networks controlling dehiscence act on different fruit types, which could allow us to control pod dehiscence (Lewis *et al*. 2006, Bennett *et al*. 2011).

To explore the effects of structure differentiation on pod shatter, we compared anatomical patterns during fruit development of different pod shatter fruit types in *S. alba*, *B. napus*, *B. rapa*, and *B. carinata*. To gain insight into the molecular basis of dehiscence variation, we identified the homologs of fruit valve margin identity genes (*i.e.*, *SHP1*, *SHP2*, *IND*, and *ALC*), valve gene *FUL*, an upstream gene of valve margin identity genes *AG*, secondary cell wall-related gene *NST1*, and seed abscission-related gene *STK* from these four species and compared their gene expression patterns during fruit development. Cellular and molecular comparisons between these taxa were performed during fruit development and among species.

Materials and methods

Plants and sample collection: *Brassica napus* L. cv. Zhongshuang10*, Brassica rapa* L. cv. Qingyuan, *Brassica carinata* L., and *Sinapis alba* L. were grown in soil under natural conditions in the Wuhan University in China. Individual flowers on the primary inflorescence were hand pollinated and tagged to ensure the seed set and to allow the analysis and collection of material at different developmental stages as defined by Roeder and Yanofsky (2006) and slightly modified with the division of stage 17 into stages 17A and 17B. Siliques were collected at stages 13, 16, 17A, 17B, 18, and 19 from randomly selected 5 individual plants, and seeds were immediately dissected out using a dissecting needle, and silique walls were frozen in liquid nitrogen for total RNA extraction. Young

leaves were harvested at the anthesis stage and immediately placed into liquid nitrogen for later total RNA extraction. For each sample, the experiment was repeated three times, which generated three biological replicates to minimize variation during processing.

Histological staining: Tissue taken from the middle portion of the fruit was fixed in 75 % (v/v) ethanol and 25 % cold acetate acid (v/v) for 12 h and subsequently dehydrated through an ethanol series. Transverse paraffin-embedded sections (8 or 10 μm thick) from different fruit developmental stages were prepared with an *RM2245* rotary microtome (*Leica Biosystems*, Nussloch, Germany) as described Liljegren *et al*. (2000).

To observe the changes of the valve margin during fruit development, the sections were stained using Safranin *O* and/or Fast Green as described Wu *et al*. (2006). To observe lignified cells, mature silique (stage 17B) sections were stained with 2 % (m/v) phloroglucinol in 95 % (v/v) ethanol and 50 % (v/v) HCl for 5 min as described Liljegren *et al*. (2000). Thickened and lignified cell walls were stained red.

To estimate the number of cell layers that composed the fruit pericarp, at least 10 transects were drawn from the epidermis to the endodermis of the pericarp for each section and the number of cells counted manually. The average value of at least four different fruit samples is presented. Light microscopy images were obtained using a *BX51* microscope and the images were captured with a *DP72* digital camera (*Olympus*, Tokyo, Japan).

RNA isolation, cDNA synthesis, and cloning homologous genes: The total RNA was isolated from siliques and leaves using a *TRIzol* reagent (*Invitrogen*, Carlsbad, CA, USA) based on the manufacturer's protocol. The total RNA was treated with RNase-free DNase I (*Fermentas*, MD, USA) to digest genomic DNA contamination. The RNA was quantified using *BioPhotometer plus* (*Eppendorf*, Hamburg, Germany) and quality was checked using *Agilent 2100 Bioanalyzer* (Palo Alto, USA) following the manufacturer's instructions. The total RNA was reverse-transcribed into the first-strand cDNA by *oligo-(dT)*$_{18\text{-}25}$ and *M-MLV* reverse transcriptase (*Promega*, Madison, WI, USA). The resulted cDNA was stored at -20 °C for later use.

We isolated the homologs of eight candidate pod shattering-related genes of *Arabidopsis*, including *SHP1*, *SHP2*, *IND*, *ALC*, *FUL*, *AG*, *NST1*, and *STK*, *via* polymerase chain reaction (PCR), from *S. alba*, *B. napus*, *B. rapa*, and *B. carinata*, respectively, and named them according to standardization which suggested Østergaard *et al*. (2008). Initially, primers were designed using the *Primer 5* software based on nucleotide sequences available in GenBank (Table 1). The primers were designed using exon regions in order to achieve fragments of 100 - 200 bp. The primers were evaluated for the presence of a single fragment in PCR using *NCBI Primer-Blast*. The products were loaded on an agarose gel and extracted using *AxyPrep*™ DNA gel extraction kits (*AxyGEN*, Silicon Valley, USA) according to the manufacturer's instructions. The extracted products were cloned with a *Dual Promoter TA Cloning*® kit (*Invitrogen*). The clones were sequenced with M13F and M13R. The sequencing results were manually edited in *MacVector v. 11.1* (*MacVector Inc.*, Cary, NC, USA) and the candidate genes were initially analyzed using *BLASTN* database (http://www.ncbi. nlm.nih.gov/BLAST/). Multiple alignments of the candidate gene sequences were carried out using *Clustal X* (Fig. 1 Suppl.). To confirm gene homology, phylogenetic analyses were then conducted. Phylogenetic trees were generated using the neighbor-joining approach (1 000 bootstrap replicates, a bootstrap value > 50 %) in *MEGA v. 4.0* after making the multiple alignment of nucleotide sequences with the *Clustal X* software. The neighbor-joining trees and GenBank accession numbers of all genes used in our study are shown in Fig. 2 Suppl. and Table 1 Suppl.

Real-time quantitative polymerase chain reaction was carried out in duplicates using *SYBR Green I* as fluorescent detection dye and they were performed on an *ABI StepOne*™ RT-qPCR system (*Applied Biosystems*, Foster City, USA). The RT-qPCR was performed in a volume of 20 mm^3, including 1 mm^3 of cDNA, 0.6 mm^3 of each reverse and forward primers (10 μM), 7.4 mm^3 of double distilled H_2O, 0.4 mm^3 of Rox, and 10 mm^3 of a qPCR master-mixture (*Thunderbird SYBR* qPCR mix, Toyobo, Japan). In every RT-qPCR run, *ACT2/7* was used as internal control to normalize for variation in the amount of a cDNA template (Girin *et al*. 2010). The primers of *ACT2/7* are also referred as in Girin *et al*. (2010), and those of *NST1* are referred as in Mitsuda and Ohme-Takagi (2008). Appropriate primers for partial fragments of *SHP1*, *SHP2*, *IND, ALC*, *FUL*, *AG*, and *STK* were designed using the *DNAMAN 6.0* software (*Lynnon-Biosoft*, San Ramon, USA) and *Primer 5* to avoid detecting other homologous sequences. Primers for RT-qPCR reactions are listed in Table 1. The RT-qPCR program consisted of the first step of denaturation and Taq activation (95 ºC for 10 min) followed by 40 cycles (90 ºC, 1 s; 62 °C, 1 min) with a single fluorescent reading taken at the end of each cycle. Melting curves were examined to ensure the specificity of amplification and lack of primer dimers which produced a single product. A negative control containing no template cDNA was subjected to the same procedure to rule out possible contamination. Relative quantification analysis was performed by a relative standard curve according to threshold values (C_T) generated from the machine's analysis. After the experiment, the C_T number was extracted for both a reference gene and a target gene with an auto baseline and a manual threshold of 0.4594.

We calculated relative expression based on delta C_T calculation (Livak and Schmittgen 2001). We first normalized all reference gene (REF in short) transcript levels relative to a standard (*ACT2/7*) using the formula ΔC_T (REF) - ΔC_T (*ACT2/7*). We next calculated an average ΔC_T value for each tissue. The expression of

SalS.AG at stage 16 with the highest relative expression (the lowest ΔC_T value) was used as standard for comparison of expression levels. We then calculated relative expression levels using the equation $100 \times 2^{-[\text{average } \Delta CT \text{ (REF)} - \text{average } \Delta CT(SalS.AG)]}$. Reported values are means of four independent replicates. Error bars indicate standard deviation (SD).

Statistical analysis: The RT-qPCR gene expression was quantified using the $2^{-\Delta\Delta Ct}$ comparative methods. Results are presented as means ± SD of two independent experiments with two biological replicates. The significant differences ($P \leq 0.05$) between means were determined by one-way *ANOVA* followed by Tamhane's T2 post hoc test using the *IBM SPSS Statistics 20* (*SPSS commercial software*, SPSS Inc., Chicago, IL, USA) software.

Table 1. Primers used in identification of homologs and RT-qPCR studies.

Name	Primer sequences (5'-3')	Comments
ACT2/7-F	5'-TTCAATGTCCCTGCCATGTA-3'	primers for PCR amplifying and RT-qPCR
ACT2/7-R	5'-GAGACGGAGGATAGCGTGAG-3'	
SHP1-F	5'-CTGAATGTCCCGAATCTGC-3'	primers for PCR amplifying
SHP1-R	5'-GTGTGATGCTGAAGTTGCC-3'	
SHP1-F	5'-CTGAATGTCCCGAATCTGC-3'	RT-qPCR for gene expression
SHP1-R	5'-GCCCTCGTTATCTTCTCCAC-3'	
SHP2-F	5'-GCAGGAAGCGAGTGTGAT-3'	primers for PCR amplifying
SHP2-R	5'-GTTTTGGTCGGAGGAGTT-3'	
SHP2-F	5'-CAACAAGGGACGGTTTACG-3'	RT-qPCR for gene expression
SHP2-R	5'-TTGGTCGGAGGAGTTCTGAT-3'	
IND-F	5'-TTCAAGAACTTGGTGTAGCG-3'	primers for PCR amplifying and RT-qPCR
IND-R	5'-TCGGCGTAGAGAAAGGATAA-3'	
ALC-F	5'-GTTTCTTACGCCGCTTGT-3'	primers for PCR amplifying and RT-qPCR
ALC-R	5'-TTCTCGTTGATCTTGCTCCT-3'	
FUL-F	5'-TGAGAAGCGTATTATTGTGAT-3'	primers for PCR amplifying and RT-qPCR
FUL-R	5'-CAAGGCAAGAGTTGAGGTA-3'	
AG-F	5'-GAGTCTGATGCCAGGAGGAT-3'	primers for PCR amplifying and RT-qPCR
AG-R	5'-CTGCGGATGAGTAATGGTGAT-3'	
NST1-F	5'-CACCGGAGATGGAGCTATG-3'	primers for PCR amplifying and RT-qPCR
NST1-R	5'-CTCTCTTTCCCTCCATTTCCGTTA-3'	
STK-F	5'-GAGTCTCCCATTAGATTCCTGT-3'	primers for PCR amplifying
STK-R	5'-CAGAAGTTGCCCTCATCG-3'	
STK-F	5'-AATCGTTTGGATCTGTTGCC-3'	RT-qPCR for gene expression
STK-R	5'-GTTGCCCTCATCGTCTTCTC-3'	

Results

Development of the *Brassicaceae* fruit after fertilization is divided into seven ontogenetic stages based on Roeder and Yanofsky (2006). In *Arabidopsis*, the flower begins to open and self-pollinate at stage 13. After gynoecium fertilization, small fruits form at stage 16, elongate, and increase in width to the mature form at stage 17. These fruits then turn yellow at stage 18 and dry at stage 19 (Roeder and Yanofsky 2006). To explore the effects of structure differentiation on pod shatter, we studied developmental processes and compared the anatomical patterns of the fruit dehiscence zone from stage 13 (the flower is about to open and the gynoecium has not been pollinated) to 19 in *S. alba*, *B. napus*, *B. rapa*, and *B. carinata* (Fig. 1). Mature fruits (stage 18) from the four species showed similar widths (approximately 4 - 5 mm) but significantly different lengths; mature *S. alba* fruits were approximately 2.2 cm long, whereas those of *B. carinata* and *B. rapa* were approximately 4.6 cm long, and mature *B. napus* fruit could be approximately 7.5 cm long (Fig. 1).

Cross-sections of the valve margin regions during fruit development were observed using Safranin *O* / Fast Green staining (Figs. 2, 3, and 3 Suppl.). Within the pre-fertilized and just-fertilized gynoecium, the carpel wall showed similar tissue patterns in the four species, and in all species, it differentiated into the exocarp (a layer of small, almost isodiametric cells), mesocarp with thin-walled mesophyll cells, and two layers of endocarp (stage 13; Fig. 3 Suppl.). A site consisting of thin-walled, almost isodiametric parenchyma cells with meristematic activity (where the dehiscence zone would form) was located at the valve margin. After gynoecium fertilization, the exocarp cells expanded and transformed into long rectangular cells (Fig. 3 Suppl.). The endocarp cells in *B. rapa* were relatively large, and the inner tangential side was rough compared to the other three species at stages 13 and 16. There were 8 - 9 layers of mesocarp cells in *B. napus*, *B. rapa*, and *B. carinata*, whereas 11 - 12 layers of

cells were observed in *S. alba* (Fig. 3 Suppl.). Only the main vascular trace surrounded by the replum and several scattered small vascular elements in the mesocarp showed red staining (Fig. 3 Suppl.). The narrow strips of cells at the valve margin developed more slowly and were much smaller than neighboring cells in the valves and replum; however, it was not possible to distinguish any putative dehiscence zone in fruit during the early developmental stages (Fig. 3 Suppl.).

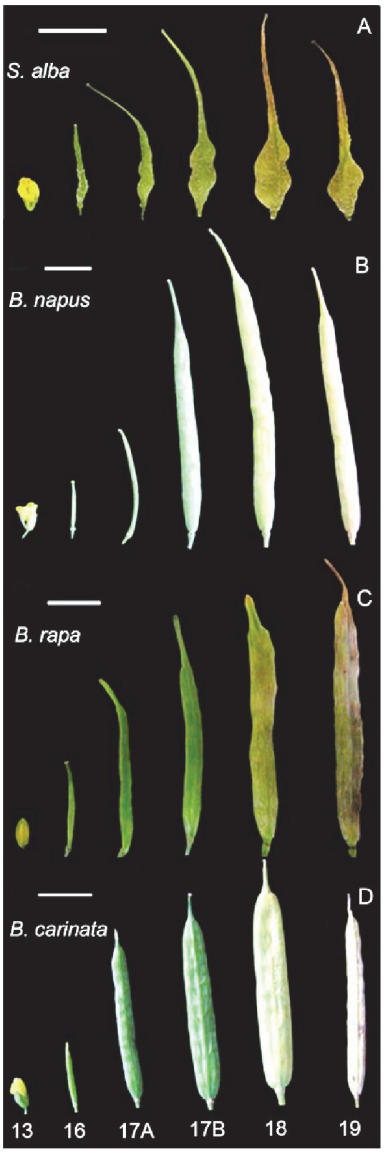

Fig. 1. Developmental stages of flowers and fruits of *Sinapis alba* (*A*), *Brassica napus* (*B*), *B. rapa* (*C*), and *B. carinata* (*D*). *Scale bars* = 1 cm.

A secondary wall deposition in the layer of valve margin cells adjacent to the valves as well as in the inner layer endocarp *b* was first detected at stage 17A. Meanwhile, a layer of small thin-walled cells stained blue with fast green, which revealed that the valve margin had differentiated into two cell types and the dehiscence zone (DZ) had formed (Fig. 2*A*,*D*,*G*,*J*). The dehiscence zone was further delineated by extensive secondary wall thickening and lignification of endocarp *b* cells and replum vascular cells. Concomitant with the onset of pericarp lignification, the dehiscence zone was fully formed at stage 17B (Fig. 2*B*,*E*,*H*,*K*) when the fruit reached a full length. The fruit was mature and green at stage 17 when the DZ was enclosed by thickened tissue, and the cells showed progressive reductions in both volume and organelle content. The *B. napus* fruit gradually turned yellow after stage 18 when separation of dehiscence zone cells was observed, resulting in breakdown of the middle lamella and loss of cellular cohesion (Fig. 2*F*). Secondary wall thickening and lignin deposition in the vascular bundles constructing the replum in *B. napus* (Fig. 2*D* - *F*) were greater than those in the shatter-resistant species *B. carinata* (Fig. 2*J* - *L*), *B. rapa* (Fig. 2*G* - *I*), and *S. alba* (Fig. 2*A* - *C*). The fruit valves of *S. alba* (Fig. 2*A* - *C*), *B. rapa* (Fig. 2*G* - *I*), and *B. carinata* (Fig. 2*J* - *L*) showed similar developmental patterns to *B. napus* (Fig. 2*D* - *E*); however, there were several differences in the DZ structure and developmental characteristics. In *B. rapa*, the inner and outer tangential walls of endocarp *b* thickened although the radial walls remained thin at stage 17A (Fig. 2*G*). In addition, there were multiple layers of non-lignified separation layer cells at the valve margin in *B. napus* (Fig. 2*D* - *F*), whereas only a single layer of non-lignified separation layer cells was observed at the valve margin in *S. alba* (Fig. 2*C*), *B. rapa* (Fig. 2*H*,*I*), and *B. carinata* (Fig. 2*K*,*L*). Vascular bundles in the replum were larger in the mature *B. napus* fruit (Fig. 2*E*,*F*) compared to the other three species (Fig. 2*B*,*C*,*H*,*I*,*K*,*L*). Separation of dehiscence zone cells occurred in the *B. napus* fruit (Fig. 2*F*), whereas it was not observed in the other three species at stage 18 (Fig. 2*C*,*I*,*L*).

At stage 19, the valves begin to separate from the replum and fell from the silique. The walls of exocarp cells and a portion of mesocarp cells neighboring the lignified valve margin layer and endocarp *b* were stained red, and were also observed during fruit development (Fig. 3). The separation layer between cells became more distinct at stage 19 siliques in *S. alba*, *B. napus*, and *B. rapa* (Fig. 3*A* - *C*), whereas the cells present at the separation layer position had a different morphology in *B. carinata*: a portion of the separation layer cells toward the inner valve margin were lignified and the valves and the replum were held together by a lignified bridge as indicated by the *black arrow* in Fig. 3*D*.

As lignification in specific tissues during fruit development plays an important role in fruit dehiscence, we investigated lignification patterns at the dehiscence zone of mature fruits of the four species using phloroglucinol, a lignin-specific histological stain, which stained lignified cell walls red. In fruit stage 17 B, transverse sections of the central region showed that *S. alba* (Fig. 4*A*) and *B. carinata* (Fig. 4*D*) fruits contained an enlarged replum, whereas the size of the outer replum of *B. napus* (Fig. 4*B*) and *B. rapa* (Fig. 4*C*) was

significantly reduced leaving the valves in close contact. Transverse sections of mature fruits from four species showed a similar lignification pattern at the valve-replum region; *i.e*., lignification of valve margin cells adjacent to the separation layer, lignification of vascular bundle cells in the replum, and lignification of endocarp *b* layer cells (Fig. 4). However, subtle but significant differences were observed. Two small and tightly packed layers of lignified valve margin cells were observed in *S. alba* (Fig. 4*A*), *B. rapa* (Fig. 4*C*), and *B. carinata* (Fig. 4*D*) fruits, whereas a single lignified valve margin cell was located between the central replum and the valve margin in *B. napus* (Fig. 4*B*). In contrast, 2 - 3 layers of small non-lignified cells formed the separation layer, and more cell separation sites were observed between lignified replum cells in *B. napus* (Figs. 2*D* - *F*, 3*B*, and 4*B*). The shatter-susceptible plant, *B. napus*, contained a large vascular trace that lignified and covered approximately 80 % of the replum (Fig. 4*B*). The shatter-resistant plants, *B. rapa* (Fig. 4*C*) and *B. carinata* (Fig. 4*D*), contained an increased number of parenchymatous cells adjacent to the vascular traces, and the indehiscent plant, *S. alba* (Fig. 4*A*), had the lowest lignin accumulation within the main vascular trace in the replum. Furthermore, vascular cells within the replum were much denser in *B. napus* (Figs. 3*B* and 4*B*) than in *S. alba* (Figs. 3*A* and 4*A*). In

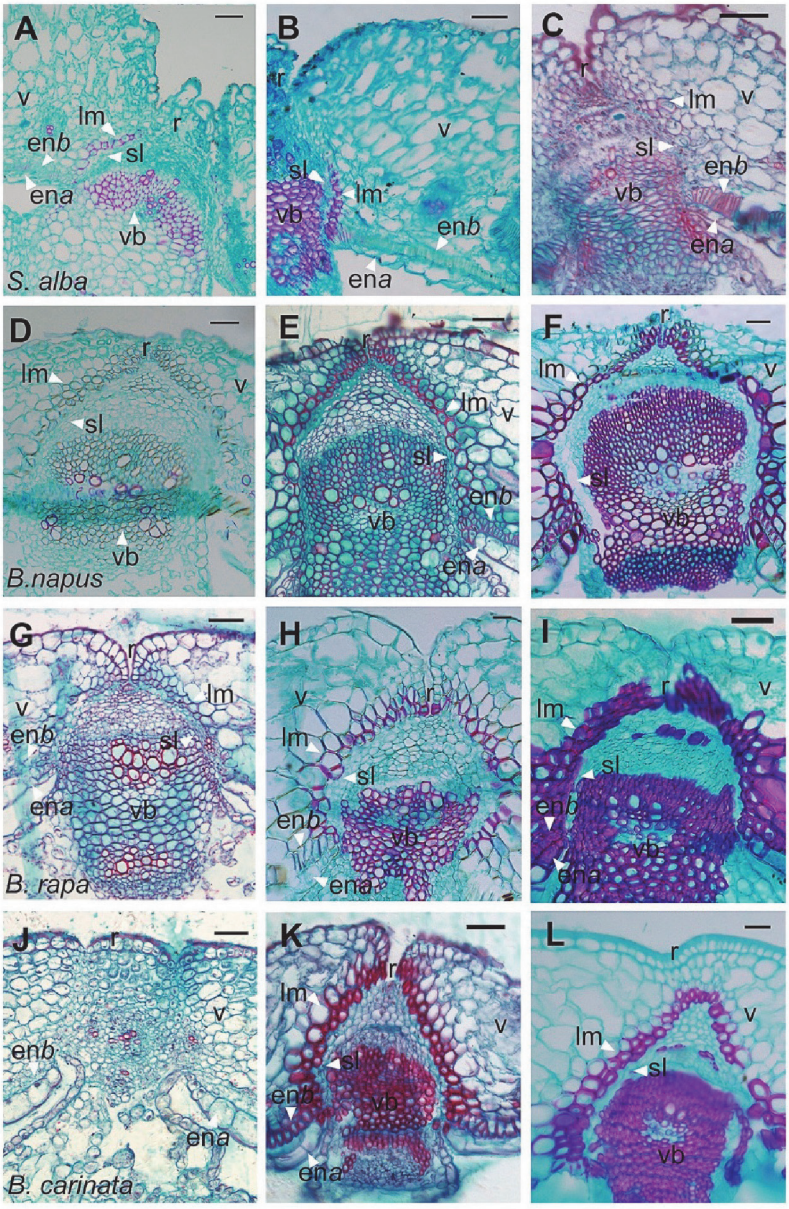

Fig. 2. Transverse sections showing a mature fruit in stage 17A (*A*, *D*, *G*, *J*), stage 17B (*B*, *E*, *H*, *K*), and stage 18 (*C*, *F*, *I*, *L*) in *S. alba* (*A* - *C*), *B. napus* (*D* - *F*), *B. rapa* (*G* - *I*), and *B. carinata* (*J* - *L*). v - valve, r - replum, vm - valve margin, sl - separation layer, lm - lignified layer at the valve margin, en*b* - endocarp *b* layer, en*a* - endocarp *a* layer, vb - vascular bundle. *Scale bars* in *A*-*D*, *F*, *G*, *I*-*L* = 50 µm, in *E*, *H* = 20 µm.

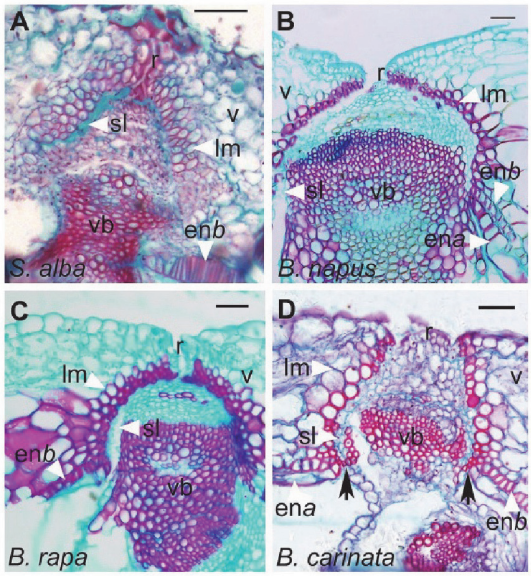

Fig. 3. Transverse sections showing a stage 19 fruit in *S. alba* (*A*),
B. napus (*B*), *B. rapa* (*C*), and *B. carinata* (*D*). The valve on the left side has already separated from the replum at the separation layer (*B* and *C*). A lignified bridge is present between the lignified valve margin cells and the lignified replum vasculature as indicated by the *black arrow* (*D*). The *white arrows* point to v - valve, r - replum, vm - valve margin, sl - separation layer, lm - lignified layer at the valve margin, en*b* - endocarp *b* layer, en*a* - endocarp *a* layer, and vb - vascular bundle. *Scale bars* = 50 μm.

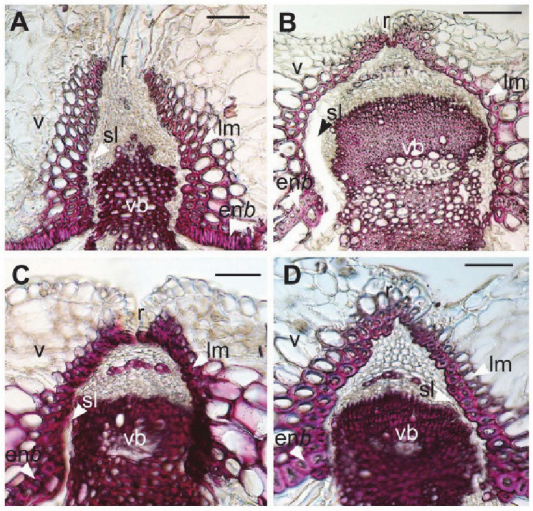

Fig. 4. Transverse sections of the midregion of stage 17B fruits of *S. alba* (*A*), *B. napus* (*B*), *B. rapa* (*C*), and *B. carinata* (*D*) stained with phloroglucinol. Lignified cell walls stained red. v - valve, r - replum, vm - valve margin, sl - separation layer, lm - lignified layer at the valve margin, en*b* - endocarp *b* layer, vb - vascular bundle. *Scale bars* = 100 μm.

addition, the cells of the endocarp *b* layer in *S. alba* were triangle shaped and more compactly arranged than those in *B. napus* and *B. rapa* (Fig. 4). Thickening mesophyll cell walls adjacent to the endocarp was also apparent. An increased lignification was observed in mesocarp cells (four/five-cell layer) around the valve margins in *B. napus* and *B. rapa* (Fig. 4*B*, *C*), whereas three layers of lignified mesocarp cells around the valve margins adjacent to endocarp *b* were observed in *S. alba* and *B. carinata* (Fig. 4*A*, *D*).

To check whether there was a correlation between the expression pattern of pod shatter-related genes and the silique morphology, we performed RT-qPCR for the homologs of *SHP1*, *SHP2*, *ALC*, *IND*, *FUL*, *AG*, *STK*, and *NST1* genes from *S. alba*, *B. napus*, *B. rapa*, and *B. carinata*. A total of 32 homologs were identified using the primers derived from *A. thaliana* and *Brassica* conserved sequences. The sequences of the candidate genes were initially analyzed using *BLASTN*, which revealed a high degree of DNA sequence similarity to the respective pod shatter-related genes from *A. thaliana* or *Brassica*. Gene identity was confirmed based on phylogenetic analyses of *AGAMOUS*, *FUL*, *bHLH*, and *NST1*-like sequences from a range of dicotyledons. Phylogenetic analyses show that all genes under study were closely related to genes from other *Brassicaceae* species indicating that they were putative homologs of the corresponding *A. thaliana* pod shatter-related genes (Fig. 2 Suppl.).

The comparisons of expression patterns of the putative fruit valve margin identity genes (*i.e.*, *SHP1*, *SHP2*, *IND*, and *ALC*), valve gene *FUL*, an upstream gene of valve margin identity genes *AG*, the secondary cell wall-related gene *NST1*, and the seed abscission-related gene *STK* in *S. alba*, *B. napus*, *B. rapa*, and *B. carinata* were analyzed in carpel/fruit walls at stages 13, 16, 17A, 17B, 18, and 19 (Fig. 1) as well as in young leaves. All genes were expressed mainly in fruit walls, and a low or no expression was observed in leaves. The only exception was *FUL* in leaves; it showed an expression comparable to carpel/fruit walls (Figs. 5 and 6).

Expressions of *Bna.SHP1*, *BraA.SHP1*, and *Bca.SHP1* were much higher than *SalS.SHP1* in the carpel walls at stage 13. Expression of *SalS.SHP1* increased rapidly at stage 16 (before dehiscence zone specification and differentiation), and then decreased, whereas *Bna.SHP1*, *BraA.SHP1*, and *Bca.SHP1* showed identical expression patterns, decreasing from stage 13 until reaching a minimum level at stages 17A/B. During later developmental stages, the expression patterns of *SalS.SHP1* were consistent with those of *BraA.SHP1* and *Bca.SHP1* which increased from stage 17B and peaked at stage 19. However, the overall expression of *SalS.SHP1* was significantly lower than in other species from stage 17A to 18. Expression of *SHP1* showed an increase in *S. alba*, *B. carinata*, and *B. rapa* fruit walls, whereas expression of *Bna.SHP1* decreased to a minimum level at stage 19. Expression of *Bca.SHP1* was 96-fold higher than that of *SalS.SHP1*, 120-fold higher than that of *BraA.SHP1*, and more than 390-fold higher than that of *Bna.SHP1* at stage

19 when the separation layer began to split between the cell layers (Fig. 5*A*).

The *SHP2* showed a higher expression in carpel walls at stage 13 compared to later stages in all four species. The *SalS.SHP2* and *Bca.SHP2* reached a lower peak level at stage 17, whereas *Bna.SHP2* and *BraA.SHP2* peaked at stage 16. The *SalS.SHP2*, *Bca.SHP2*, and *BraA.SHP2* showed an increased expression at stage 19 in contrast to *Bna.SHP2*.

Expression of *SalS.SHP2* was 3.8-fold higher than that of *Bna.SHP2* at stage 19, and *Bca.SHP2* expression was approximately 10-fold higher than that of *Bna.SHP2* at stage 19. Overall, expressions of *SalS.SHP1*, *SalS.SHP2*, *BraA.SHP1*, *BraA.SHP2*, *Bca.SHP1*, and *Bca.SHP2* increased in the fruit walls at stage 19, whereas expressions of *Bna.SHP1* and *Bna.SHP2* in the fruit wall of *B. napus* remained relatively stable (Fig. 5*B*).

The *SalS.IND*, *BraA.IND*, and *Bca.IND* genes showed relatively lower expressions at stage 13 compared to stage 16, whereas *Bna.IND* showed a very high expression at

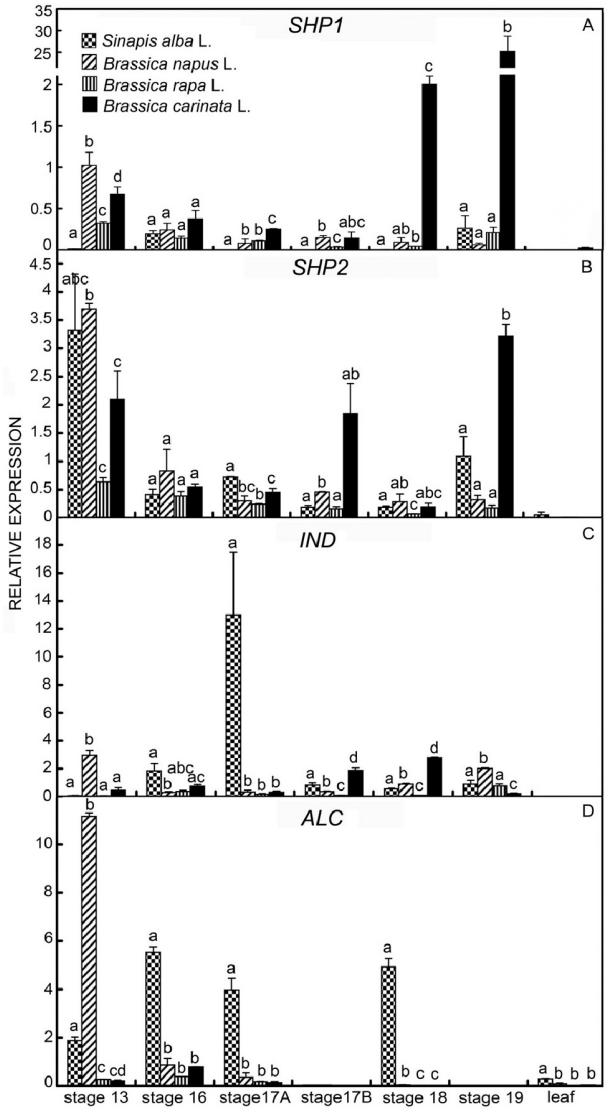

Fig. 5. RT-qPCR showing expression of valve margin identify genes *SHP1* (*A*), *SHP2* (*B*), *IND* (*C*), and *ALC* (*D*) in different developmental stages of fruits and young leaves of *S. alba*, *B. napus*, *B. rapa* and *B. carinata*. A gene *ACT2/7* was used as internal control. The *vertical columns* indicate relative expression (means ± standard deviations of two independent experiments with two biological replicates). The significant differences in expression of each gene among the four species at the same development stage were determined by one-way *ANOVA* followed by Tamhane's T2 post hoc test. Means marked with the same *letter* are not significantly different ($P > 0.05$).

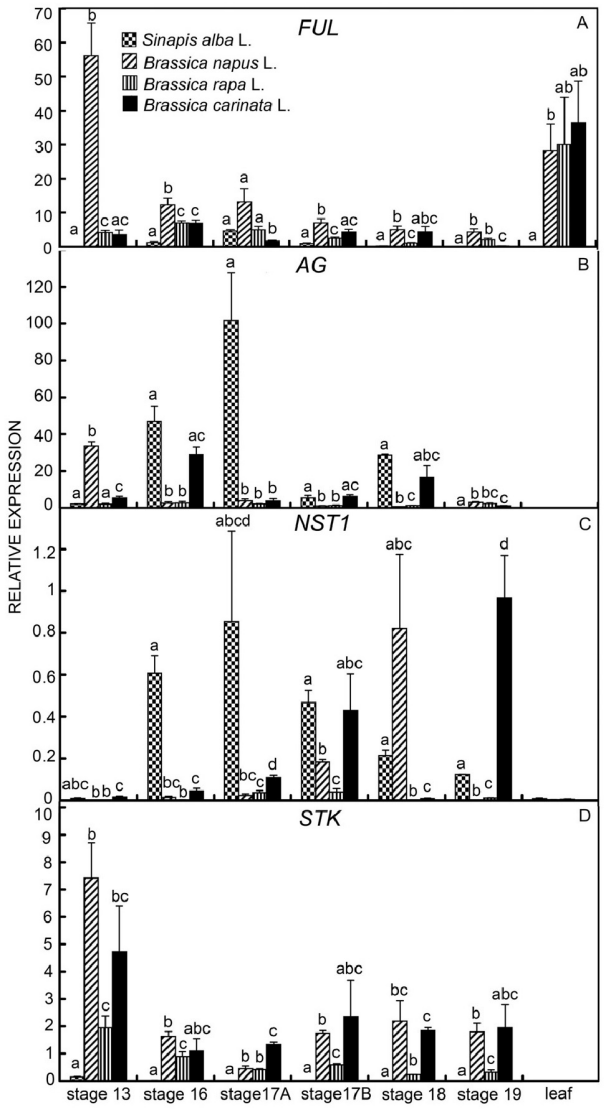

Fig. 6. RT-qPCR showing expression of *FUL* (*A*), *AG* (*B*), *NST1* (*C*), and *STK* (*D*) in different developmental stages of fruits and young leaves of *S. alba*, *B. napus*, *B. rapa* and *B. carinata*. A gene *ACT2/7* was used as internal control. The *vertical columns* indicate relative expression (means ± standard deviations of two independent experiments with two biological replicates). The significant differences in expression of each gene among the four species at the same development stage are determined by one-way *ANOVA* followed by Tamhane's T2 post hoc test. The means marked with the same *letter* are not significantly different ($P > 0.05$).

stage 13; it then decreased by approximately 10-fold by stage 16. Expression of *SalS.IND* increased significantly in the fruit walls to levels much higher than those of *Bna.IND*, *Bca.IND*, and *BraA.IND* at stage 17A when the valve margin began to specify different cell fates. There was a slight increase in expression of *SalS.IND* at stage 19, and expression of *Bna.IND* showed a gradual increase from stage 16 peaking at stage 19. Expressions of *BraA.IND* and *Bca.IND* showed two peaks; a low peak at stage 16 (similar to *SalS.IND*) and a high peak at stage 18/19. Overall, expression of *IND* showed a strong and rapid increase in the fruit walls from stage 16 and increased expression at later mature stages when the fruit was about to dehiscence (Fig. 5*C*).

Expression of *ALC* in the fruit walls in these four species was high during the early stages (13 - 17A) and low (or absent) during later developmental stages. The overall expression of *SalS.ALC* in the fruit walls of *S. alba* was considerable higher than in the other three species, excluding expression at stage 13 and in young leaves. During stage 13, expression of *Bna.ALC* in the carpel walls was higher than in the other species. After gynoecium fertilization, expression of *SalS.ALC* significantly increased (particularly at stage 18), *SalS.ALC* expression was 126.4-fold, 8649.1-fold, and 835.5-fold higher than those of *Bna.ALC*, *BraA.ALC*, and *Bca.ALC*, respectively. The *SalS.ALC* showed high expressions at stages 13, 16, 17A, and 18. Low expressions of *SalS.ALC* were detected at stages 17B and 19. The *Bna.ALC* showed higher expressions at stages 13, 16, and 17A compared with later stages. Expression of *BraA.ALC* showed an identical pattern to *Bca.ALC* with an initial increase followed by a decrease (Fig. 5*D*).

The overall expression of *Bna.FUL* in the fruit walls was higher than in the fruit walls of *S. alba*, *B. rapa*, and *B. carinata*. Expression of *SalS.FUL* was significantly lower compared to other species and peaked at stage 17A. The *Bna.FUL* showed a low peak at stage 17A when the dehiscence zone differentiated, and then expression decreased after stage 17B. Expression of *BraA.FUL* was highest at stage 16, then decreased to stage 18 and slightly increased at stage 19. Expression of *Bca.FUL* peaked at stage 17A and reached the lowest level at stage 19. Similar expressions of *Bca.FUL* and *BraA.FUL* were observed at stages 13 and 16. Overall, *FUL* showed high expressions at stages 16 and 17A in the fruit walls of all four species when the dehiscence zone was about to differentiate. In addition, young leaves showed fairly high *Bca.FUL*, *Bna.FUL*, and *BraA.FUL* expressions (Fig. 6*A*).

Expression of *Bna.AG* was significantly higher than those of *SalS.AG*, *BraA.AG*, and *Bca.AG* at stage 13. The expression patterns were similar among these four species after stage 13, and the first increase occurred at stage 16 or 17A and the second at stage 18 or 19. At stage 17A, expression of *SalS.AG* in the fruit walls was approximately 26-fold higher than that of *Bna.AG*, 47-fold higher than that of *BraA.AG*, and 27-fold higher than that of *Bca.AG*. There was a small peak in *SalS.AG* expression at stage 18, and it was similar to the expression pattern of *SalS.ALC*. Expression of *Bna.AG* peaked at stage 13 and showed two smaller peaks at stages 17A and 19. Expression of *BraA.AG* overlapped with *Bca.AG* expression and showed a considerable induction at stage 16 followed by a decrease. However, *BraA.AG* expression increased at stage 19, whereas *Bca.AG* increased at stage 18. The overall expression of *SalS.AG* was significantly higher than those of *AG* in the other species, and *Bna.AG* (as well as *BraA.AG*) showed relatively lower expressions during fruit development (Fig. 6*B*).

Expression of *NST1* within these four species was fairly low in the carpel walls at stage 13 before gynoecium fertilization, and then increased markedly from stage 16 before secondary wall formation. During stage 16, expression of *SalS.NST1* was significantly higher than those of *Bna.NST1*, *BraA.NST1*, and *Bca.NST1*. In stage 17A, *SalS.NST1* expression peaked after establishment of the dehiscence zone and before secondary cell wall thickening was evident. The expression pattern was consistent with the results of *SalS.IND* experiments described above (Fig. 6C). Stage 17B expressions of *SalS.NST1* and *Bca.NST1* were approximately 10-fold higher than those of *Bna.NST1* and *BraA.NST1*. The overall expression of *SalS.NST1* was much higher than those of the other species during early fruit development (stages 16 and 17 A/B). Expression of *SalS.NST1* gradually decreased during the late stages in the mature fruits. Expression of *Bna.NST1* peaked, whereas expressions of *SalS.NST1*, *BraA.NST1*, and *Bca.NST1* decreased at stage 18, at which time the secondary walls were thickened and accumulation of lignin increased. During stage 19, *Bca.NST1* expression peaked, whereas the others decreased to their lowest levels. Overall, *NST1* expression increased from stage 16 before the secondary cell walls began to differentiate and lignin deposition began. Importantly, *SalS.NST1* expression peaked at stage 17A, *Bna.NST1* at stage 18, *BraA.NST1* at stage 17B, and *Bca.NST1* at stage 19 (Fig. 6*C*).

The overall expression of *SalS.STK* was low compared to the other three species during fruit development. Expressions of *Bna.STK*, *BraA.STK*, and *Bca.STK* were much higher at stage 13 than at stage 16. During later developmental stages, expression of *STK* in the four species remained relatively stable and showed a slight increase at stage 17B (Fig. 6*D*).

Discussion

Pod morphological characteristics, such as pod length, wall thickness, beak length, and vascular tissue size, are related to pod shatter resistance (Summers *et al*. 2003). However, Wang *et al*. (2007) demonstrated that pod shatter resistance is not significantly associated with plant morphological characteristics, excluding pod length in

B. napus, *B. juncea*, and *S. alba*. According to our anatomical analysis, the fruit wall of *S. alba* was thicker than those of *B. napus*, *B. rapa*, and *B. carinata*, as the mesocarp of *S. alba* was 11 - 12 layers thick, whereas those of the other three species were 8 layers thick. Short and thick-walled pods may reduce physical stress on the dehiscence zone in *S. alba*, which influences fruit splitting. However, pod shatter resistance may be associated more with tissue-specific architecture and physiology of the dehiscence zone and its surrounding area (Wang *et al*. 2007, Mummenhoff *et al*. 2009). Valve margins differentiate into a lignification layer and a separation layer, which facilitates fruit opening and the efficient release of seeds. The separation layer secretes hydrolytic enzymes to degrade cell walls and allows cell-cell separation to occur (Ogawa *et al*. 2009). As lignin deposition within specific fruit tissue layers is a common method for fruit dehiscence and seed dispersal, the lignified valve margin layer is believed to provide tension to facilitate the opening mechanism (Mitsuda and Ohme-Takagi 2008, Zhao and Dixon 2011, Seymour *et al*. 2013). Multiple layers of lignified valve margin cells were observed in *S. alba*, *B. rapa*, and *B. carinata*, whereas a single layer of cells was observed in *B. napus*. It is possible that shatter resistance is associated with increased lignification at the junction of the valves in the replum. A striking phenomenon in *B. carinata* was that a lignified bridge of cells was present between the lignified inner valve cell layers and the lignified replum vasculature at stage 19, which prevented the valves detached from the replum, resulting in more rigid siliques in *B. carinata* than in *B. napus* and *B. rapa*. In addition, more separation layer cells between the lignified valve margin cells and the replum were observed in *B. napus* compared to the other three species, which may facilitate pod shatter by splitting the separation layer and increasing the number of parenchymal cells. Furthermore, the degree of lignin deposition in vascular bundle cells forming the replum was highest in the shatter-susceptible plant *B. napus*, lower in *B. rapa* and *B. carinata*, and lowest in *S. alba*. Thus, the size of the vascular tissue in the replum may be associated with pod shatter resistance, which is consistent with previous studies by Child *et al*. (2003) and Wang *et al*. (2007). Tension in the pod is believed to be caused primarily by lignification of the endocarp cells surrounding the dehiscence zone (Spence *et al*. 1996). Spence *et al*. (1996) demonstrated that endocarp *b* is not completely lignified in *B. juncea*, which reduces the shatter tendency. Cells of the endocarp *b* layer in *B. napus*, *B. rapa*, and *B. carinata* were similar, and their cell walls were heavily thickened. Secondary wall thickening and lignin deposition in the endocarp *b* cells first occurred in the inner and outer tangential walls, and was then detected in the endocarp *b* cells in the radial walls. For *S. alba*, cells of endocarp *b* were long with anticlinal packing and were relatively large compared to the other species. The activities of *SHP1*, *SHP2*, *IND*, *ALC*, and *FUL* are each required for the differentiation of the endocarp *b* layer (Liljegren *et al*. 2004) although the precise roles of these antagonistic factors in endocarp *b* development are unclear. In conclusion, fruit morphology, such as fruit length and fruit wall thickness, as well as tissue-specific differences in the separation layer, lignified valve margin layer, vascular bundle of the replum, and lignin deposition between the four species of the plant family *Brassicaceae*, may be associated with pod shatter resistance.

It is possible that indehiscence in some species of *Brassicaceae* may be due to modifications in the valve margin genetic pathway (Mummenhoff *et al*. 2009). Four of the genes (*FUL*, *IND*, *ALC*, and *RPL*) have been investigated in *Brassica* with a focus on the conservation of dehiscence rather than the divergence of indehiscence (Østergaard *et al*. 2006, Wu *et al*. 2006, Hua *et al*. 2009, Girin *et al*. 2010, Arnaud *et al*. 2011). We isolated homologs of eight fruit developmental genes (*SHP1*, *SHP2*, *IND*, *ALC*, *FUL*, *AG*, *NST1*, and *STK*), which are known to be essential for pod shatter in *Arabidopsis*, from the shatter-susceptible plant *B. napus*, shatter-resistant plants *B. rapa* and *B. carinata*, and *S. alba* which shows no pod shatter except that due to an external force. The expression studies in the four species revealed conserved expression patterns in the fruit-patterning pathway in *Arabidopsis*; however, divergent or modified expressions of pod shatter-related genes during fruit development may result in different pod shatter phenotypes.

Specification and differentiation of the valve margin began at stage 16 or 17. This process requires expressions of valve margin identity genes *IND*, *SHP1*, *SHP2*, *ALC*, and their inhibitor *FUL* (Ferrándiz *et al*. 2000, Rajani and Sundaresan 2001, Liljegren *et al*. 2000, 2004). Three important up-regulations of expression were observed in pre-fertilization at stage 13, stages 16 and 17A, and stage 19. The highest or relatively higher expression of all genes studied commenced at stage 16 or 17A, suggesting that a similar (or identical) dehiscence zone specification pathway was shared between species (Ferrándiz *et al*. 2000, Liljegren *et al* 2000, 2004, Østergaard *et al*. 2006). In *B. napus*, *Bna.FUL* showed a significantly higher expression compared to the homologs in other species, especially in *S. alba*, during fruit development. Short and thick-walled pods of *S. alba* were reminiscent of the short *ful* mutant fruit (Ferrándiz *et al*. 2000) and suggest that the low expression of *SalS.FUL* might be associated with the short pod of *S. alba*. The high expression of *Bna.FUL*, the low expressions of *Bna.IND* and *Bna.ALC*, the low expression of *SalS.FUL*, as well as the high expressions of *SalS.IND* and *SalS.ALC* suggest that the function of *FUL* in repressing the expression of *IND* and *ALC* in *Arabidopsis* appears to be conserved in *Brassica* (Fig. 5; Ferrándiz *et al*. 2000, Liljegren *et al*., 2004). The *STK* showed similar expression patterns in all four species examined; *NST1* expression in the four species peaked when fruit tissue identity was established after stage 17A/B, and expression of *ALC* in the fruit walls within these four taxa was high during the early stages (13-17A) and low during the late mature developmental stages. These results are suggestive of conserved expression patterns of the fruit-patterning pathway within the four

species compared to *Arabidopsis*.

However, divergence in expression patterns among these species was observed, especially between pod shatter-susceptible *B. napus* and shatter-resistant *S. alba*. For *S. alba*, the expressions of *SalS.AG*, *SalS.IND*, *SalS.ALC*, and *SalS.NST1* were significantly higher during fruit development compared to the other species. The up-regulated expression of *IND* in the *ful* mutant is involved in regulating ectopic valve lignification (Liljegren *et al*. 2004). The high number of lignified margin layers in the *S. alba* fruit appears to be that the valve cells adopted a valve margin fate. The increased *SalS.IND* expression might be correlated with the increased size of the lignification layer in valves. The *ALC* is a key regulator that drives separation layer formation, and Lenser and Theißen (2013) identified *ALC* as a negative regulator of *IND*, whereas *IND* acts in the separation layer as activator of *ALC* together with auxin and gibberellin (Sorefan *et al*. 2009, Arnaud *et al*. 2010). Expression of *Bna.ALC* in *B. napus* was mainly observed in the carpel walls at stage 13 and in the fruit walls at stages 16 and 17A, which is similar to the results of Hua *et al*. (2009). Reduced *ALC* expression leads to the absence of non-lignified small separation layer cells in *alc* mutants (Rajani and Sundaresan 2001). The overall expression of *Bna.ALC* in the carpel/fruit walls of pod shatter-susceptible *B. napus* was higher than those of *BraA.ALC* and *Bca.ALC* in pod shatter-resistant species *B. rapa* and *B. carinata*, respectively, showing that the higher *Bna.ALC* expression might be associated with the increased number of separation layer cells present at the valve margin in *B. napus*. Reduced *ALC* expression leads to ectopic lignification of those cells that normally form the separation layer in *alc* mutants (Rajani and Sundaresan 2001), which is similar to the lignified bridge present between the lignified valve and the lignified replum vascular bundle in *B. carinata*, thus we conclude that the lignified bridge in *B. carinata* might be associated with the reduced *ALC* expression. In addition, *SalS.SHP1* and *SalS.STK* showed the significantly lower expressions than those in the other species at stage 17 and during the fruit developmental stages, respectively. The expression patterns of valve margin identity genes in pod shatter-resistant *S. alba* in the dehiscence zone partially agreed with recent studies showing that the valve margin identity genes *SHP1*, *SHP2*, *IND*, and *ALC* are not expressed in the valve margin of *Cakile lanceolata* (Avino *et al*. 2012) and *Lepidium* (Mühlhausen *et al*. 2013) indehiscent fruits lacking the dehiscence zone. The significantly lower expression of *SalS.SHP1* at stage17 and *SalS.SHP2* at stage 17B in *S. alba* compared to other species might be an important characteristic related to differences in pod shatter resistance. The *stk* mutant in *Arabidopsis* that does not produce a clear abscission zone does not perform seed detachment (Bennett *et al*. 2011, Martinez-Andujar *et al*. 2012) suggesting that the low STK expression in *S. alba* might be associated with a reduction of seed shattering.

Furthermore, *NST1* is responsible for secondary wall formation and acts in a partially redundant manner with *NST3* at the valve margin and endocarp cells in *Arabidopsis*, functioning after the establishment of fruit tissue identity. In *nst1* mutants, a specific loss of secondary walls is evident at valve margins, whereas *nst1 nst3* double mutants lack secondary walls in all parts of the siliques excluding vascular vessels (Mitsuda and Ohme-Takagi 2008). In our study, the overall expression of *SalS.NST1* was significantly higher than those in the other species during early fruit development (before secondary walls became evident, stages 16 and 17A/B), similar to that which has been described for the *NST1* gene of *Arabidopsis* (Mitsuda and Ohme-Takagi 2008). This expression pattern is also consistent with the results of experiment that *NST1* is expressed specifically in the endocarp and is initiated at the same time as lignin deposition in peach (Dardick *et al*. 2010). The expression pattern of *SalS.NST1* was consistent with the increased number of secondary wall cells observed in *S. alba* showing that the high level of *NST1* expression might be associated with more lignified valve margin layers. These results suggest that the indehiscent fruit phenotype in *S. alba* might involve reduced expressions of *SalS.FUL*, *SalS.SHP1*, and *SalS.STK*; however, it is possible that the increased *SalS.AG*, *SalS.IND*, *SalS.ALC* and *SalS.NST1* expression levels might be associated with the indehiscent fruit phenotype.

In conclusion, the comparisons of the anatomical patterns of the dehiscence zone and expression patterns of pod shatter-related genes during fruit development suggest that differences in the dehiscence zone and tissue-specific lignin deposition patterns may be associated with modified expression levels of the valve margin identity genes. Different expression patterns of genes involved in pod shatter among the four *Brassicaceae* species examined (especially between *B. napus* and *S. alba*) will increase our understanding of pod shatter resistance.

References

Arnaud, N., Girin, T., Sorefan, K., Fuentes, S., Wood, T.A., Lawrenson, T., Sablowski, R., Østergaard, L.: Gibberellins control fruit patterning in *Arabidopsis thaliana*. - Gene. Dev. **24**: 2127-2132, 2010.

Arnaud, N., Lawrenson, T., Østergaard, L., Sablowski, R.: The same regulatory point mutation changed seed-dispersal structures in evolution and domestication. - Curr. Biol. **21**: 1215-1219, 2011.

Avino, M., Kramer, E.M., Donohue, K., Hammel, A.J., Hall, J.C.: Understanding the basis of a novel fruit type in *Brassicaceae*, conservation and deviation in expression patterns of six genes. - Evodevo **3**: 20, 2012.

Bennett, E.J., Roberts, J.A., Wagstaff, C.: The role of the pod in seed development, strategies for manipulating yield. - New

Phytol. **190**: 838-853, 2011.
Child, R.D., Summers, J.E., Babij, J., Farrent, J.W., Bruce, D.M.: Increaced resistance to pod shatter is associated with changes in the vaslular structure in pods of a resynthesized *Brassica napus* line. - J. exp. Bot. **54**: 1919-1930, 2003.
Dardick, C.D., Callahan, A.M., Chiozzotto, R., Schaffer, R.J., Piagnani, M.C., Scorza, R.: Stone formation in peach fruit exhibits spatial coordination of the lignin and flavonoid pathways and similarity to *Arabidopsis* dehiscence. - BMC Biol. **8**: 13, 2010.
Dinneny, J.R., Yanofsky, M.F.: Drawing lines and borders: how the dehiscent fruit of *Arabidopsis* is patterned. - Bioessays **27**: 42-49, 2005.
Favaro, R.: MADS-box protein complexes control carpel and ovule development in *Arabidopsis*. - Plant Cell **15**: 2603-2611, 2003.
Ferrándiz, C.: Regulation of fruit dehiscence in *Arabidopsis*. - J. exp. Bot. **53**: 2031-2038, 2002.
Ferrándiz, C., Liljegren, S.J., Yanofsky, M.F.: Negative regulation of the *SHATTERPROOF* genes by *FRUITFULL* during *Arabidopsis* fruit development. - Science **289**: 436-438, 2000.
Girin, T., Stephenson, P., Goldsack, C.M.P., Kempin, S.A., Perez, A., Pires, N., Sparrow, P.A., Wood, T.A., Yanofsky, M.F., Østergaard, L.: *Brassicaceae INDEHISCENT* genes specify valve margin cell fate and repress replum formation. - Plant J. **63**: 329-338, 2010.
Gonzalez-Reig, S., Ripoll, J.J., Vera, A., Yanofsky, M.F., Martínez-Laborda, A.: Antagonistic gene activities determine the formation of pattern elements along the mediolateral axis of the *Arabidopsis* fruit. - PLoS Genet. **8**: e1003020, 2012.
Hua, S., Shamsi, I.H., Guo, Y., Pak, H., Chen, M., Shi, C., Meng, H., Jiang, L.: Sequence, expression divergence, and complementation of homologous *ALCATRAZ* loci in *Brassica napus*. - Planta **230**: 459-503, 2009.
Kadkol, G.P.: Brassica shatter-resistance research update. - In: Proceedings of the 16th Australian Research Assembly on Brassicas. Pp. 104-109. Ballarat, Victoria 2009.
Lenser, T., Theißen, G.: Conservation of fruit dehiscence pathways between *Lepidium campestre* and *Arabidopsis thaliana* sheds light on the regulation of *INDEHISCENT*. - Plant J. **76**: 545-556, 2013.
Lewis, M.W., Leslie, M.E., Liljegren, S.J.: Plant separation: 50 ways to leave your mother. - Curr. Opin. Plant Biol. **9**: 59-65, 2006.
Liljegren, S.J., Ditta, G.S., Eshed, Y., Savidge, B., Bowman, J.L., Yanofsky, M.F.: *SHATTERPROOF* MADS box genes control seed dispersal in *Arabidopsis*. - Nature **404**: 766-770, 2000.
Liljegren, S.J., Roeder, A.H., Kempin, S.A., Gremski, K., Østergaard, L., Guimil, S., Reyes, D.K., Yanofski, M.F.: Control of fruit patterning in *Arabidopsis* by *INDEHISCENT*. - Cell **116**: 843-853, 2004.
Livak, K.J., Schmittgen, T.D.: Analysis of relative gene expression data using real-time quantitative PCR and the 2(-Delta Delta C(T)) method. - Methods **25**: 402-408, 2001.
Martinez-Andujar, C., Martin, R.C., Nonogaki, H.: Seed traits and genes important for translational biology – highlights from recent discoveries. - Plant Cell Physiol. **53**: 5-15, 2012.
Mitsuda, N., Ohme-Takagi, M.: NAC transcription factors NST1 and NST3 regulate pod shattering in a partially redundant manner by promoting secondary wall formation after the establishment of tissue identity. - Plant J. **56**: 768-778, 2008.
Mühlhausen, A., Lenser, T., Mummenhoff, K., Theißen, G.: Evidence that an evolutionary transition from dehiscent to indehiscent fruits in *Lepidium* (*Brassicaceae*) was caused by a change in the control of valve margin identity genes. - Plant J. **73**: 824-835, 2013.
Mummenhoff, K., Polster, A., Mühlhausen, A., Theißen, G.: *Lepidium* as a model system for studying the evolution of fruit development in *Brassicaceae*. - J. exp. Bot. **60**: 1503-1513, 2009.
Ogawa, M., Kay, P., Wilson, S., Swain, S.M.: *ARABIDOPSIS DEHISCENCE ZONE POLYGALACTURONASE1* (*ADPG1*), *ADPG2*, and *QUARTET2* are polygalacturonases required for cell separation during reproductive development in *Arabidopsis*. - Plant Cell **21**: 216-233, 2009.
Østergaard, L., Kempin, S.A., Bies, D., Klee, H.J., Yanofsky, M.F.: Pod shatter-resistant *Brassica* fruit produced by ectopic expression of the *FRUITFULL* gene. - Plant Biotechnol. J. **4**: 45-51, 2006.
Østergaard, L., King, G.J.: Standardized gene nomenclature for the *Brassica* genus. - Plant Methods **4**: 10, 2008.
Pinyopich, A., Ditta, G.S., Baumann, E., Wisman, E., Yanofsky, M.F.: Unraveling the redundant roles of MADS-box genes during carpel and fruit development. - Nature **424**: 85-88, 2003.
Rajani, S., Sundaresan, V.: The *Arabidopsis* myc/bHLH gene *ALCATRAZ* enables cell separation in fruit dehiscence. - Curr. Biol. **11**: 1914-1922, 2001.
Roeder, A.H., Yanofsky, M.F.: Fruit development in *Arabidopsis*. - In: Somerville, C., Meyerowitz, E. (ed.): The Arabidopsis book. Pp 1-50. American Society of Plant Biologists, Rockville 2006.
Seymour, G.B., Østergaard, L., Chapman, N.H., Knapp, S., Martin, C.: Fruit development and ripening. - Annu. Rev. Plant Biol. **64**: 219-241, 2013.
Sorefan, K., Girin, T., Liljegren, S.J., Ljung, K., Robles, P., Galván-Ampudia, C.S., Offringa, R., Friml, J., Yanofsky, M.F., Østergaard, L.: A regulated auxin minimum is required for seed dispersal in *Arabidopsis*. - Nature **459**: 583-586, 2009.
Spence, J., Vercher, Y., Gates, P., Harris, N.: Pod shatter in *Arabidopsis thaliana*, *Brassica napus* and *B. juncea*. - J. Microscopy **181**: 195-203, 1996.
Summers, J.E., Bruce, D.M., Vancanneyt, G., Redig, P., Werner, C.P., Morgan, C., Child, R.D.: Pod shatter resistance in the resynthesized *Brassica napus* line DK142. - J. agr. Sci. **140**: 43-52, 2003.
Wang, R., Ripley, V.L., Rakow, G.: Pod shatter resistance evaluation in cultivars and breeding lines of *Brassica napus*, *B. juncea* and *Sinapis alba*. - Plant Breed. **126**: 588-595, 2007.
Wu, H., Mori, A., Jiang, X., Wang, Y., Yang, M.: The INDEHISCENT protein regulates unequal cell divistions in *Arabidopsis* fruit. - Planta **224**: 971-979, 2006.
Zhao, Q., Dixon, R.A.: Transcriptional networks for lignin biosynthesis, more complex than we thought? - Trends Plant Sci. **16**: 227-233, 2011.